

ELECTRONIC SUPPLEMENTARY INFORMATION

Effective hydrodeoxygenation of biomass-derived oxygenates into unsaturated hydrocarbons by MoO₃ using low H₂ pressures

Teerawit Prasomsri, Tarit Nimmanwudipong and Yuriy Román-Leshkov*

Department of Chemical Engineering, Massachusetts Institute of Technology, Cambridge MA, 02139

1. Experimental

Materials

Acetone (99.5 wt%, Macron), 2-hexanone (98 wt%, Sigma-Aldrich), cyclohexanone (99.8 wt%, Sigma-Aldrich), anisole (>99 wt%, Fluka), 2-methylfuran (99 wt%, Aldrich), and 2,5-dimethylfuran (99 wt%, Aldrich) were used as purchased. H₂ (99.999%, Airgas) and He (99.998%, Airgas) were used as a co-reactant in the reaction experiments, and as an inert carrier gas, respectively. Catalysts used were Molybdenum(VI) oxide (\geq 99.5%, Sigma-Aldrich), Vanadium(V) oxide (\geq 99.6%, Sigma-Aldrich), Copper(II) oxide (nanopowder, $<$ 50 nm, Sigma-Aldrich), Iron(III) oxide (nanopowder, $<$ 50 nm, Sigma-Aldrich), and Tungsten(VI) oxide (99.9%, Sigma-Aldrich). Prior to the experiment, the catalysts were calcined at 873 K (heating rate of 10 K/min) for 3 h under air flow.

Characterization

The powder X-ray diffraction (PXRD) pattern of the MoO₃ was recorded on a Bruker D8 Discover diffractometer, equipped with a Cu K α radiation. The surface area was determined by nitrogen adsorption/desorption experiment using a Quantachrome Autosorb iQ automated gas sorption system. Prior to the experiment, the samples were degassed at 623 K for 1 h, and surface areas were calculated using the BET method [1]. XPS spectra were collected using a PHI Versaprobe II equipped with a multichannel hemispherical analyser and aluminium anode X-ray source operating at 100 W with a 100- μ m beam scanned over a 1.4-mm line across the sample surface. A dual-beam charge neutralization system was used with an electron neutraliser bias of 1.2 eV and an Argon ion beam energy of 10 eV. The coke deposited during reaction was analysed by TGA.

Catalytic testing

The catalytic reaction experiments were conducted in a continuous tubular flow reactor (O.D. = 0.95 cm, wall thickness = 0.089 cm). The reactor was mounted in an insulated single-zone furnace (850W/115V, Applied Test Systems Series 3210). A thermocouple (Omega, model TJ36-CAXL-116u) was used to measure the temperature in a well mounted slightly downstream of the catalyst bed. In each experiment, the packed catalyst bed in the reactor consisted of catalyst (20–300 mg) mixed with inert sand (Mallinckrodt). The bed thickness was typically 5 cm long and situated in the middle of the furnace. The catalyst was pre-reduced in flowing H₂ (70 mL/min) at 673 K (heating rate of 10 K/min) for 1 h prior to the start of reactant feeds.

Liquid reactants were introduced into the reactor by using a syringe pump (Harvard Apparatus, model 703005). Carrier He gas and co-reactant H₂ gas were mixed with vaporised reactants at the inlet of the reactor. Each experiment was typically carried out at 673 K and atmospheric pressure. In some experiments, H₂/He concentrations were adjusted at constant total gas flow rate of 70 mL/min to investigate effect of H₂ partial pressure.

The space–time (W/F), expressed in $\text{g}_{\text{Cat}}/(\text{mmol}_{\text{Feed}} \cdot \text{h}^{-1})$, is defined as the ratio between the mass of the catalyst and the molar feed rate of the reactants.

The reactor effluent lines were heated at 473 K to prevent the condensation of products, which were directly analysed by an online GC (Agilent Technologies, model 7890A) equipped with a DB-5 column (Agilent, 30 m × 0.25 mm id, 0.25 μm). The GC parameters used for the analysis were as follows: injection temperature 543 K; split ratio 1:100. The temperature program started at 308 K and held for 6 minutes; then the temperature was increased at 20 K/min to 533 K, followed by a 7-min hold. The product identification was performed by using a mass selective detector (MSD, Agilent Technologies, model 5975C).

2. Theoretical Methods

In this work, a Mo_3O_9 cluster was used as a model cluster representing the MoO_3 surface. Density functional calculations (DFT) were performed using the Gaussian 09 program [2] with the unrestricted B3LYP functional with the LANL2DZ effective core potential (ECP) basis set for Mo and the 6-311+G(d,p) basis set for C, H and O. This level of theory was used for both structure optimization and energy calculation. Transition state searching was performed with the TS algorithms followed by frequency calculations to verify first-order saddle points. The calculation method used in this work was reliable and compatible with other previous studies. [3]

3. Weisz–Prater Criterion for Internal Diffusion

Internal effectiveness factor for a first-order reaction in a spherical catalyst pellet

$$\eta = \frac{3}{\phi_1^2} (\phi_1 \coth \phi_1 - 1) \quad (\text{Eq-1})$$

Weisz–Prater parameter:

$$C_{WP} = \eta \phi_1^2 = \frac{-r_A(\text{obs}) \rho_c R^2}{D_e C_{As}} \quad (\text{Eq-2})$$

where ρ_c = Density of catalyst particle, R = particle radius, D_e = Effective diffusivity, C_{As} = surface concentration

	Measured rate (obs) ^a (mol/g _{cat} .S) × 10 ³	Pellet Radius (mm)
Run#1	1.407	0.230 (35-40 mesh) ^b
Run#2	1.461	0.053 (< 140 mesh) ^c

^a Reaction conditions: T = 673 K, P_{Total} = 1.013 bar (0.048 bar P_{Acetone}, 0.965 bar P_{H₂}), W/F = 0.0061 g/(mmol.h⁻¹), TOS = 0.25 h.

^b A larger size of catalyst particle prepared for the purpose of mass-transfer analysis

^c The typical size of catalyst particle used in the regular experiment

Combining (Eq-1) and (Eq-2)

$$\frac{-r_A(\text{obs}) \rho_c R^2}{D_e C_{As}} = \eta \phi_1^2 = 3(\phi_1 \coth \phi_1 - 1) \quad (\text{Eq-3})$$

Applying (Eq-3) to Runs#1 and #2, and take the ratio, then the terms ρ_c , D_e , and C_{As} cancel because the runs were carried out under identical conditions.

$$\frac{-r_{A2} R_2^2}{-r_{A1} R_1^2} = \frac{\phi_{12} \coth \phi_{12} - 1}{\phi_{11} \coth \phi_{11} - 1} \quad (\text{Eq-4})$$

The Thiele modulus:

$$\phi_1 = R \sqrt{\frac{-r_{As} \rho_c}{D_e C_{As}}} \quad (\text{Eq-5})$$

Taking the ratio of the Thiele moduli for Runs#1 and #2

$$\frac{\phi_{11}}{\phi_{12}} = \frac{R_1}{R_2} \quad (\text{Eq-6})$$

$$\text{or } \phi_{11} = (R_1/R_2) \phi_{12} = (0.230 \text{ mm})/(0.053 \text{ mm}) \phi_{12} = 4.381 \phi_{12} \quad (\text{Eq-7})$$

Substituting for ϕ_{11} in (Eq-4) and evaluating $-r_A$ and R for Runs#1 and #2

$$\left(\frac{1.461 \times 10^{-3}}{1.407 \times 10^{-3}} \right) \left(\frac{0.053}{0.230} \right)^2 = 0.054 = \frac{\phi_{12} \coth \phi_{12} - 1}{(4.381 \phi_{12}) \coth(4.381 \phi_{12}) - 1} \quad (\text{Eq-8})$$

Solving (Eq-8)

$$\phi_{12} = 0.18 \quad \text{for } R_2 = 0.053 \text{ mm,} \quad \text{then}$$

$$\phi_{11} = 4.381 \quad \phi_{12} = 0.79 \quad \text{for } R_1 = 0.230 \text{ mm}$$

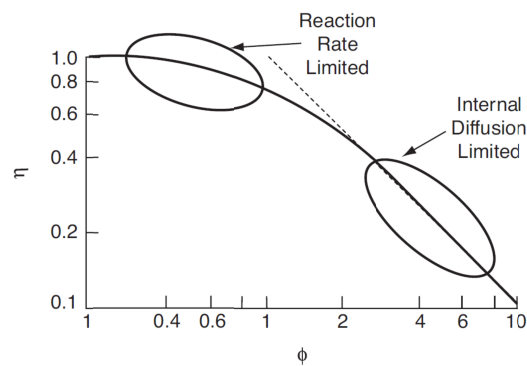
Substituting for the obtained ϕ_{12} and ϕ_{11} in (Eq-1) and evaluating the corresponding effectiveness factors

For R_2 :

$$\eta = \frac{3}{\phi_{12}^2} (\phi_{12} \coth \phi_{12} - 1) = \frac{3}{(0.18)^2} (0.18 \coth(0.18) - 1) = 0.998$$

For R_1 :

$$\eta = \frac{3}{\phi_{11}^2} (\phi_{11} \coth \phi_{11} - 1) = \frac{3}{(0.79)^2} (0.79 \coth(0.79) - 1) = 0.961$$



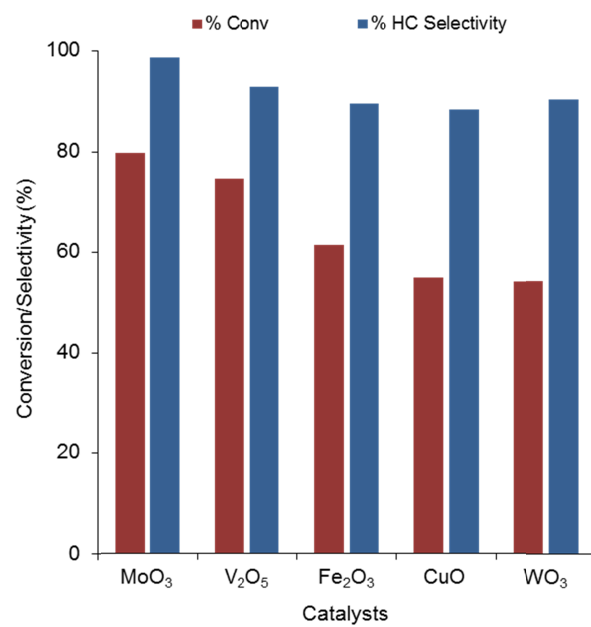
The typical size of catalyst particles used in this work is $\sim 0.053 \text{ mm} (< 140 \text{ mesh})$. The corresponding effectiveness factors suggest that the reaction is not controlled by the internal diffusion (i.e., $\eta > 0.95$)

4. HDO Activities on Various Metal Oxide Catalysts

Table S1 Conversion and product distribution of acetone on various metal oxide catalysts. Reaction conditions: T = 673 K, P_{Total} = 1.013 bar (0.040 bar P_{Acetone}, 0.973 bar P_{H₂}), TOS = 0.25 h.

Catalyst	MoO ₃	V ₂ O ₅	Fe ₂ O ₃	CuO	WO ₃
Conversion (C-mol%)	79.9	74.6	61.4	54.9	54.2
Selectivity to HCs (C-mol%)	98.2	92.8	89.5	88.3	90.3
Yields (C-mol%)					
Propylene	48.5	18.9	15.5	13.4	13.2
Butenes	6.9	6.4	5.1	5.0	6.2
Pentenes	1.5	1.9	1.9	1.7	1.8
Hexenes	19.5	28.1	23.7	20.5	19.1
Alkylbenzenes	2.1	13.9	8.7	7.9	8.7
Hexanone	1.4	5.4	6.4	6.4	5.3
S _{BET} ² (m ² /g)	11.5	8.7	53.5	15.8	11.4
W/F ($\times 10^4$ g/(mmol.h) ⁻¹) ^a	147	194	31	107	148
Specific rate (mmol/m ² /h)	14.2	13.3	10.9	9.8	9.7

^a The W/F was adjusted in order to keep the catalytic surface area of each catalyst the same.



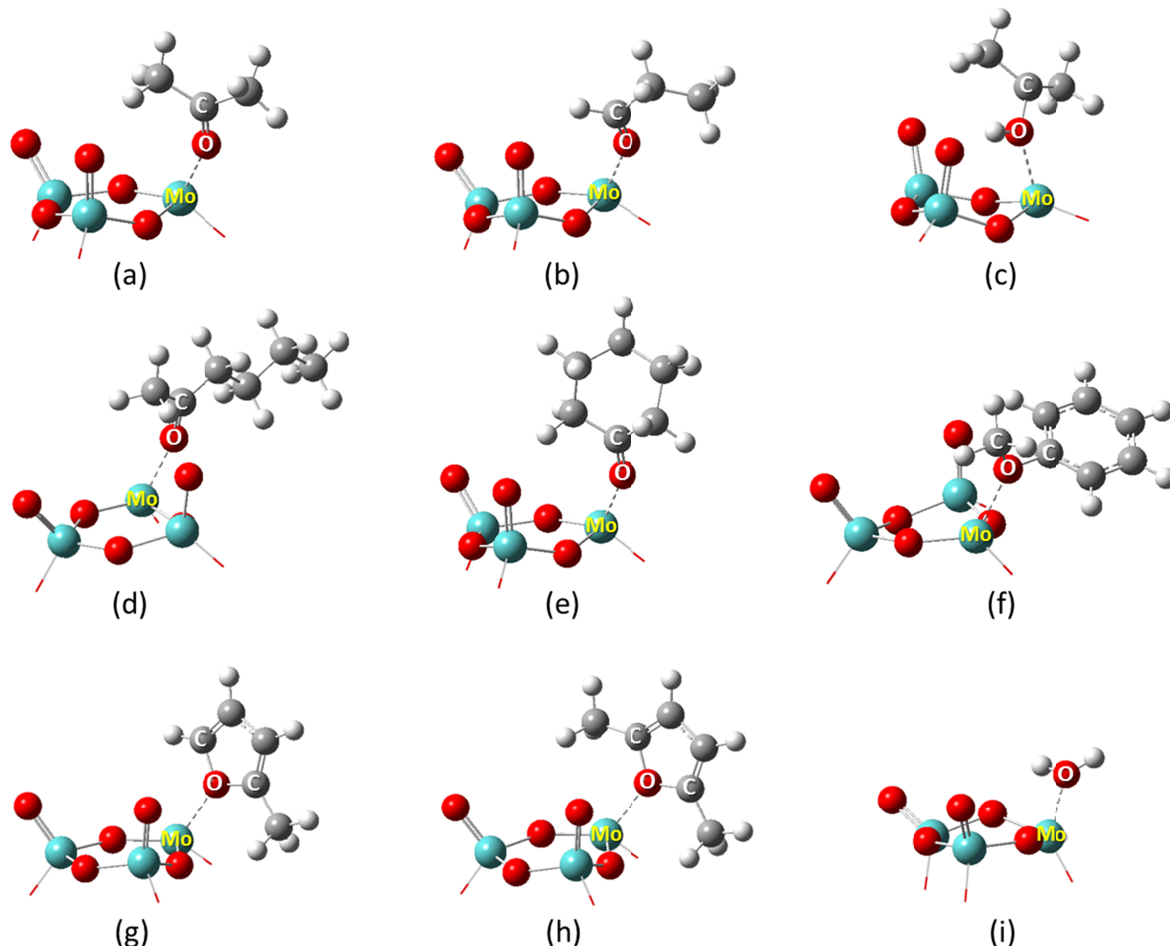
5. Reactivity Comparison of Various Oxygenates on MoO₃

Table S2 Conversion and product distribution of oxygenated compounds on MoO₃ catalysts at conversion < 30%.
 Reaction conditions: T = 673 K, P_{Total} = 1.013 bar (0.032 bar P_{Feed}, 0.196 bar P_{H₂}, balance He), TOS = 1 h.

Feed	Acetone	2-Hexanone	Cyclohexanone	Anisole	2-Methylfuran	2,5-Dimethylfuran
Conversion (C-mol%)	22.1	14.2	26.7	7.7	7.3	6.9
Selectivity to HC _s	67.9	81.7	56.6	80.5	94.5	100.0
Yields (C-mol%)						
<i>Hydrocarbons</i>						
Propylene	9.8	0.0	0.0	0.0	0.6	0.8
Butenes	1.4	0.0	0.0	0.0	0.3	0.3
Pentenes	0.0	0.0	0.0	0.0	4.5	0.0
Pentadienes	0.0	0.0	0.0	0.0	1.5	0.0
Hexenes	0.8	9.8	0.0	0.0	0.0	2.8
Hexadienes	2.3	1.8	0.0	0.0	0.0	3.0
Cyclohexene	0.0	0.0	9.9	0.0	0.0	0.0
Cyclohexadiene	0.0	0.0	1.8	0.0	0.0	0.0
Benzene	0.0	0.0	3.4	5.4	0.0	0.0
Toluene	0.0	0.0	0.0	0.8	0.0	0.0
Alkylbenzenes	0.7	0.0	0.0	0.0	0.0	0.0
<i>Oxygenates</i>						
Methylanisole	0.0	0.0	0.0	0.4	0.0	0.0
Pantanone	0.0	0.0	0.0	0.0	0.4	0.0
Hexenone	7.1	2.6	0.0	0.0	0.0	0.0
Cyclohexenone	0.0	0.0	4.0	0.0	0.0	0.0
Phenol	0.0	0.0	7.6	1.1	0.0	0.0
W/F (x10 ⁴ g/(mmol.h ⁻¹))	32.6	27.4	23.0	31.1	36.1	36.0

6. Adsorption of Oxygenated Compounds on the Reduced MoO₃ (Mo₃O₈ cluster)

Table S3 The calculated adsorption energies and optimised structures of adsorbing oxygenated compounds on Mo₃O₈ clusters: a) acetone, b) propanal, c) *i*-propanol, d) 2-hexanone, e) cyclohexanone, f) anisole, g) 2-methylfuran, h) 2,5-dimethylfuran, and i) water.



Model	Compound	Heat of adsorption (kJ/mol)	Mo–O distance (Å)	C–O distance ^a (Å)
(a)	acetone	-131.2	2.034	1.246 (+0.035)
(b)	propanal	-121.2	2.054	1.240 (+0.034)
(c)	<i>i</i> -propanol	-133.2	2.204	1.410 (+0.025)
(d)	2-hexanone	-137.3	2.041	1.246 (+0.034)
(e)	cyclohexanone	-188.6	2.037	1.447 (+0.032)
(f)	anisole	-90.3	2.136	1.445 (+0.051) ^b
(g)	2-methylfuran	-59.6	2.202	1.407 (+0.039) ^b
(h)	2,5-dimethylfuran	-60.8	2.207	1.416 (+0.044) ^b
(i)	water	-97.5	2.149	n/a

^a the numbers in the parentheses refer to the increase of bond length upon the adsorption as compared to those of the isolated molecules; ^b average bond lengths

7. Effect of Hydrogen Pressures and Water Contents

Table S4 Effect of H₂ partial pressures and water contents on acetone conversion and product distribution. Reaction conditions: T = 673 K, P_{Total} = 1.013 bar, TOS = 1 h, W/F (wrt. acetone) = 0.037 g/(mmol.h⁻¹).

Acetone:Water (w/w)	10:0			8:2			6:4		
Acetone pressure (bar)	0.048	0.048	0.048	0.048	0.048	0.048	0.048	0.048	0.048
Water pressure (bar)	0.000	0.000	0.000	0.039	0.039	0.039	0.104	0.104	0.104
H ₂ pressure (bar)	0.193	0.482	0.965	0.185	0.463	0.926	0.172	0.431	0.861
Conversion (C-mol%)	60.7	77.7	96.0	44.1	64.4	90.2	31.0	50.6	73.3
Yields (C-mol%)									
Hydrocarbons									
Propylene	26.7	44.2	62.4	22.3	39.9	60.3	19.2	36.7	53.7
Butene	5.6	6.4	5.6	6.4	5.8	5.7	2.5	2.1	1.9
Pentenes	1.0	1.3	3.0	0.2	1.3	3.0	0.3	0.8	1.1
Hexenes	10.9	15.3	22.5	6.3	8.5	18.4	3.3	5.7	13.4
Hexadiene	7.3	7.0	1.4	3.4	5.9	1.7	2.2	3.4	1.9
Alkylbenzenes	4.0	2.4	1.1	1.4	1.5	1.0	0.8	0.6	0.7
Oxygenates									
Hexanone	5.2	1.2	0.2	4.2	1.4	0.2	2.8	1.2	0.6

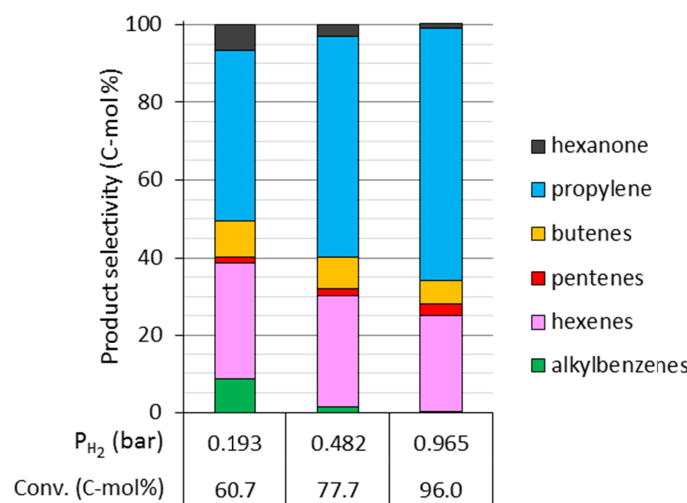


Figure S1 Comparison of product selectivity from acetone conversion at varying H₂ partial pressures. Reaction conditions: T = 673 K, P_{Total} = 1.013 bar (0.048 bar P_{Acetone}, balance He), TOS = 1 h, W/F (wrt. acetone) = 0.037 g/(mmol.h⁻¹).

8. Effect of Space Velocities on Product distribution

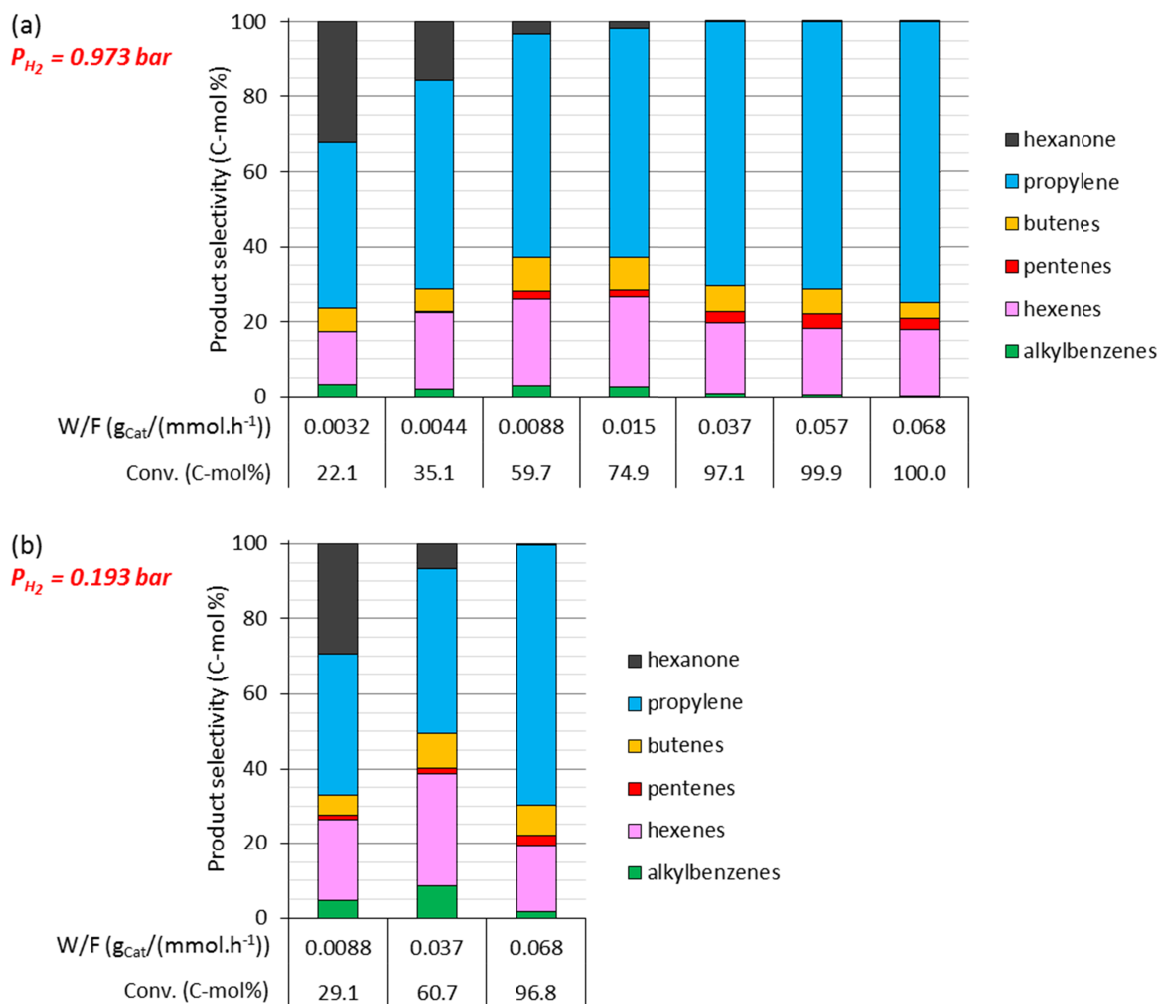
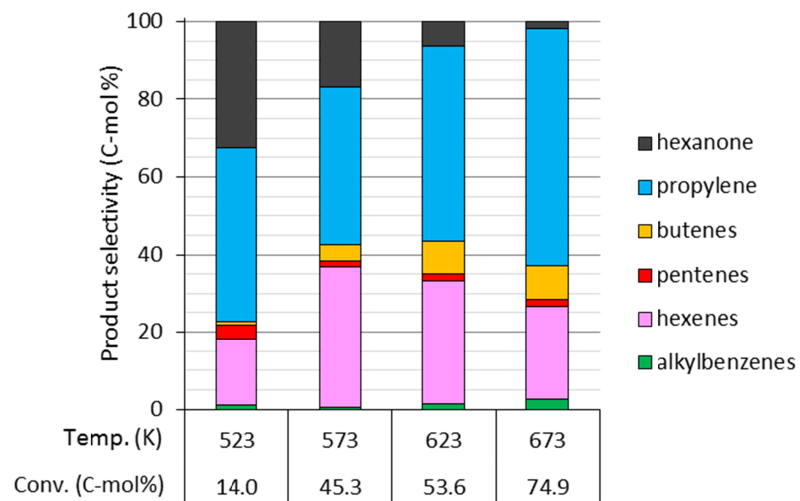


Figure S2 Comparison of product selectivity from acetone conversion at varying W/F. Reaction conditions: T = 673 K, $P_{\text{Total}} = 1.013 \text{ bar}$ (0.040 bar P_{Acetone} ; a) 0.973 bar P_{H_2} , b) 0.193 bar P_{H_2} ; balance He) TOS = 0.5 h.

9. Effect of Temperatures on HDO Performance of MoO₃

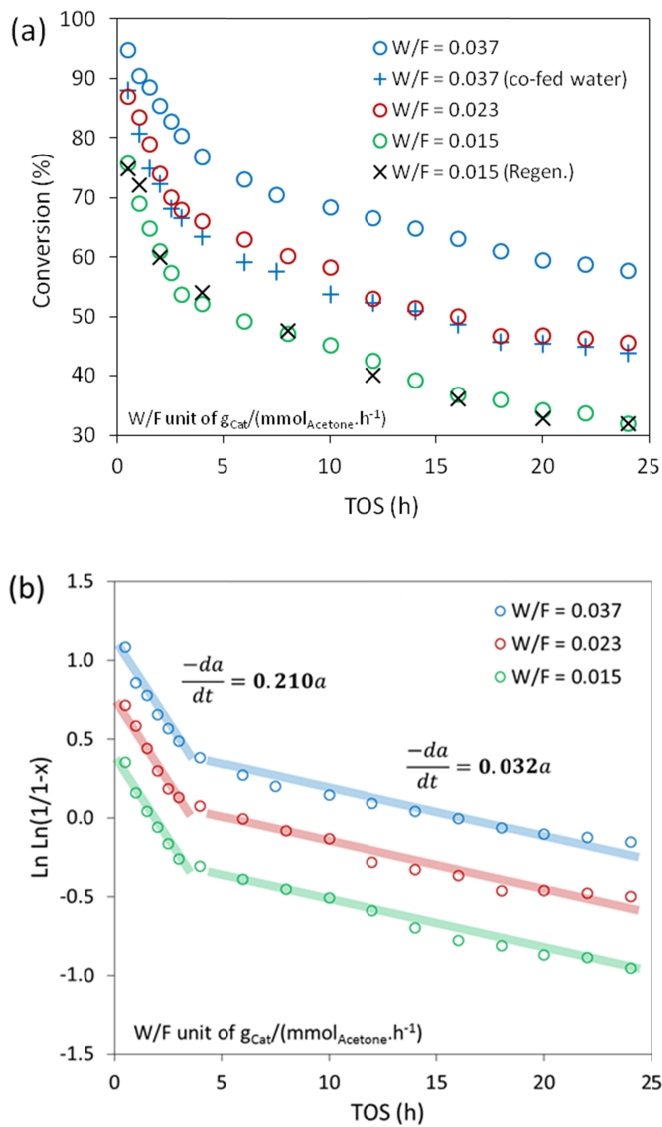
Table S5 Effect of temperatures on conversion and product distribution of acetone. Reaction conditions: P_{Total} = 1.013 bar (0.032 bar P_{Acetone}, 0.981 bar P_{H₂}), W/F = 0.015 g/(mmol.h⁻¹), TOS = 0.5 h.

Temp (K)	523	573	623	673
Conversion (C-mol%)	14.0	45.3	53.6	74.9
Selectivity to HC _s (C-mol%)	67.7	83.2	93.8	97.7
Yields (C-mol%)				
Propylene	6.3	18.4	27.0	45.8
Butenes	0.1	1.9	4.5	6.5
Pentenes	0.5	0.7	0.9	1.4
Hexenes	2.4	16.5	17.1	17.9
Alkylbenzenes	0.1	0.2	0.7	2.0
Hexanone	4.5	7.6	3.3	1.3



10. Catalyst Deactivations

Figure S3 a) Catalyst deactivation profiles from various reaction conditions, and b) representation of the fast (i.e., TOS < 4 h) and slow (i.e., TOS > 4 h) catalyst deactivation obtained from the 1st-order decay kinetic model.[4]
Reaction conditions: T = 673 K, P_{Total} = 1.013 bar (0.040 bar P_{Acetone}, 0.032 bar P_{H₂O} (for mixture feed), balance H₂).



11. PXRD Patterns of MoO₃ Samples

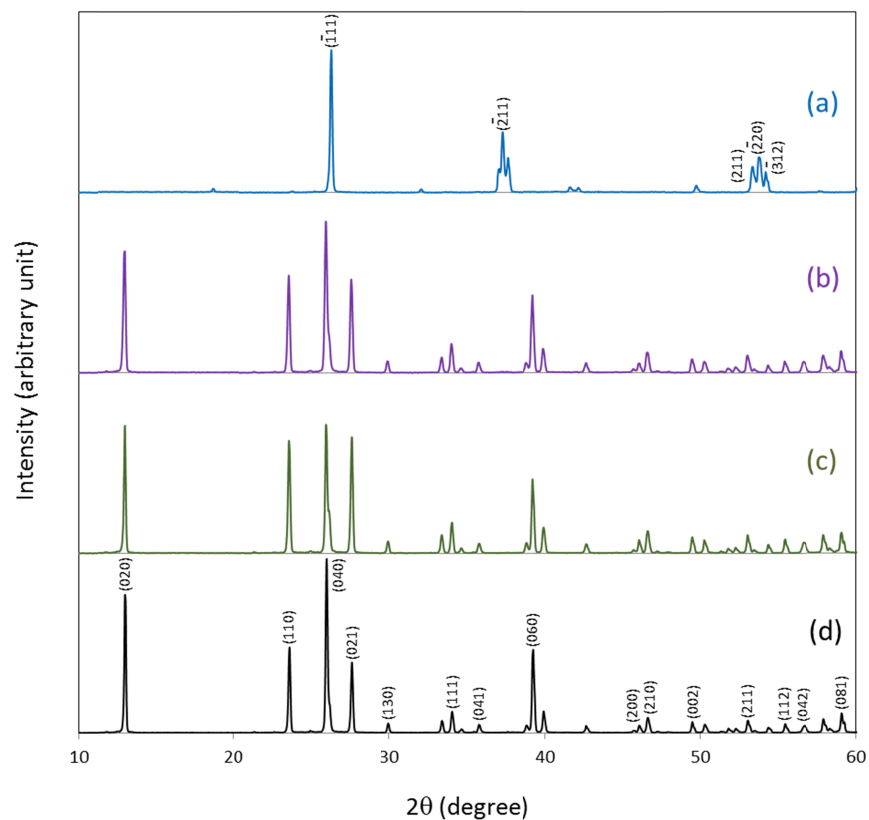


Figure S4 PXRD patterns for a) MoO₂ as-received, b) MoO₃ after reduction under H₂ at 673 K for 3 h, c) MoO₃ after calcination under air at 673 K for 3 h, and d) MoO₃ as-received.

12. XPS Binding Energies of MoO₃ Samples

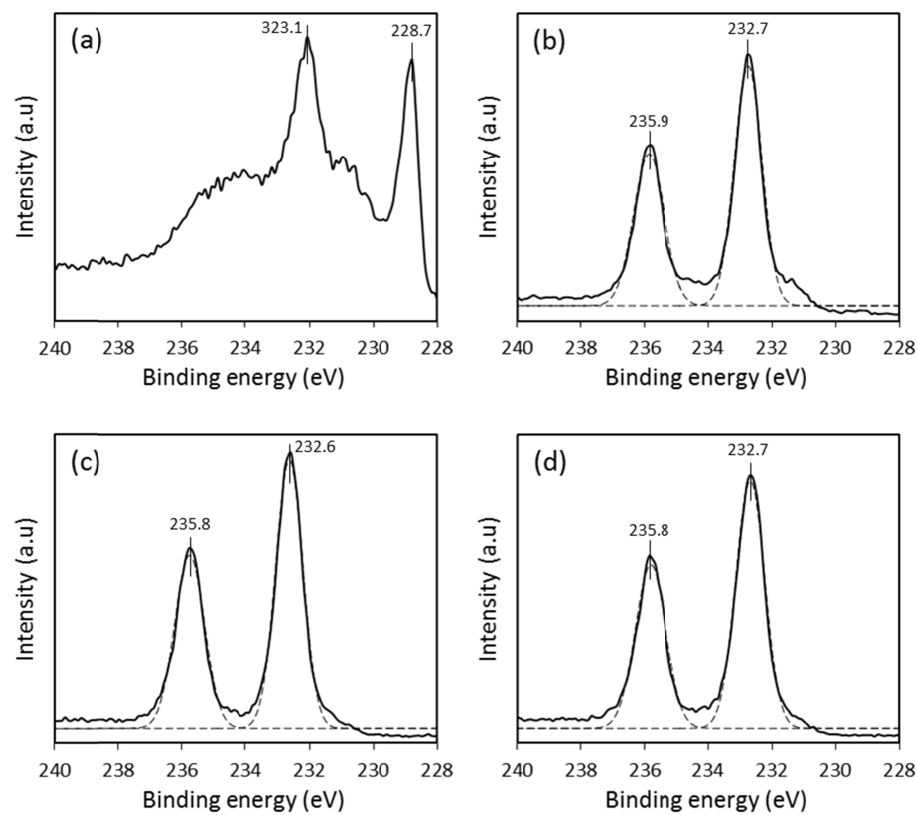


Figure S5 Mo 3d XPS binding energy regions for a) MoO₂ as-received, b) MoO₃ after reduction under H₂ at 673 K for 3 h, c) MoO₃ after calcination under air at 673 K for 3 h, and d) MoO₃ as-received.

13. Surface Coverage Calculations

Van't Hoff's equation:

$$\frac{d\ln K}{dT} = -\frac{\Delta H}{RT^2}; \text{ for the isotherm equation, } K = \exp(-\Delta G/RT)$$

where ΔG is Gibbs free energy at reaction temperature and 1 bar

R is gas constant (8.314×10^{-3} kJ/K.mol)

T is absolute temperature (K)

K is equilibrium constant

Table S6 Density of oxygen vacancy sites



Fractional surface oxygen vacancy coverage, $\theta_V = [0.25K(P_{\text{H}_2}/P_{\text{H}_2\text{O}})]^{1/3}$ [5];

$\Delta G_{\text{oxygen vacancy generation}} = 60.6 \text{ kJ/mol}$ @ 673 K (from DFT calculation);

$K_{\text{oxygen vacancy generation}} = 1.98 \times 10^5$;

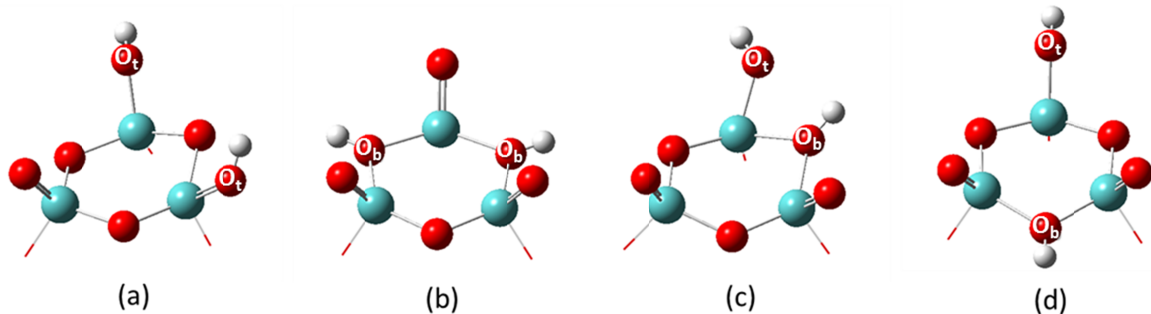
% θ_V change (from acetone:water mixture 8:2 to 6:4 w/w) = $(\theta_{V,(8:2)} - \theta_{V,(6:4)})/\theta_{V,(8:2)} \times 100\%$

Reaction conditions: T = 673 K, P_{Total} = 1.013 bar (0.048 bar P_{Acetone}), W/F (wrt. acetone) = 0.037 g/(mmol.h⁻¹).

Acetone:Water mixture (w/w)	P _{H₂} (bar)	(P _{H₂} /P _{H₂O})	$\Phi_{\text{oxy. vac.}}$
8:2 (20% water)	0.185	4.77	0.029
	0.463	11.92	0.039
	0.926	23.84	0.049
6:4 (40% water)	0.172	1.66	0.020
	0.431	4.16	0.027
	0.861	8.31	0.035

14. Adsorption of Hydrogen on MoO₃ (Mo₃O₉ cluster)

Table S7 The calculated adsorption energies and optimised structures of possible H₂ adsorption on Mo₃O₉ clusters (Mo₃O₉ + H₂ → Mo₃O₉H₂). Mo₃O₉H₂ clusters with a) two terminal hydroxyl hydrogens; b) two bridging hydroxyl hydrogens; c) with one terminal hydroxyl hydrogen and one adjacent bridging hydroxyl hydrogen; d) with one terminal hydroxyl hydrogen and one distant bridging hydroxyl hydrogen.



Model	Adsorption site ^a	Heat of adsorption (kJ/mol)
(a)	O _t , O _t	-37.5
(b)	O _b , O _b	+53.2
(c)	O _t , O _b _adjacent	-3.8
(d)	O _t , O _b _distant	-1.8

^a O_t and O_b refer to terminal and bridging oxygens, respectively.

15. Relevant Bond Dissociation Energies

Table S8 Bond dissociation energies. [6]

Group	Example compounds	Bond dissociation energy (kJ/mol)
R=O	acetone, propanal, 2-hexanone, cyclohexanone	754
R-OH	<i>i</i> -propanol	385
Ar-OH	phenol	468
R-OR	2-methylfuran, 2,5-dimethylfuran	339
Ar-OR	anisole	422
Mo=O	MoO ₃ (terminal O)	575

References (Supplementary)

- 1 S. Brunauer, P.H. Emmett and E. Teller, *J. Am. Chem. Soc.*, 1938, **60**, 309-319.
- 2 M. J. Frisch, G. W. Trucks, H. B. Schlegel, G. E. Scuseria, M. A. Robb, J. R. Cheeseman, G. Scalmani, V. Barone, B. Mennucci, G. A. Petersson, H. Nakatsuji, M. Caricato, X. Li, H. P. Hratchian, A. F. Izmaylov, J. Bloino, G. Zheng, J. L. Sonnenberg, M. Hada, M. Ehara, K. Toyota, R. Fukuda, J. Hasegawa, M. Ishida, T. Nakajima, Y. Honda, O. Kitao, H. Nakai, T. Vreven, J. A. Montgomery, Jr., J. E. Peralta, F. Ogliaro, M. Bearpark, J. J. Heyd, E. Brothers, K. N. Kudin, V. N. Staroverov, R. Kobayashi, J. Normand, K. Raghavachari, A. Rendell, J. C. Burant, S. S. Iyengar, J. Tomasi, M. Cossi, N. Rega, J. M. Millam, M. Klene, J. E. Knox, J. B. Cross, V. Bakken, C. Adamo, J. Jaramillo, R. Gomperts, R. E. Stratmann, O. Yazeyev, A. J. Austin, R. Cammi, C. Pomelli, J. W. Ochterski, R. L. Martin, K. Morokuma, V. G. Zakrzewski, G. A. Voth, P. Salvador, J. J. Dannenberg, S. Dapprich, A. D. Daniels, Ö. Farkas, J. B. Foresman, J. V. Ortiz, J. Cioslowski, and D. J. Fox, *Gaussian 09, Revision A.1*, Gaussian, Inc., Wallingford CT, 2009.
- 3 (a) D. R. Moberg, T. J. Thibodeau, F. G. Amar and B. G. Frederick, *J. Phys. Chem. C*, 2010, **114**, 13782–13795; (b) S. Pudar, J. Oxgaard, K. Chenoweth, A. C. T. van Duin and W. A. Goddard, III, *J. Phys. Chem. C*, 2007, **111**, 16405-16415; (c) R. Tokarz-Sobieraj, M. Witko, and R. Grybos, *Catal. Today*, 2005, **99**, 241-253. (d) J. Wang, Y. Su, J. Xu, C. Ye and Feng Deng, *Phys. Chem. Chem. Phys.*, 2006, **8**, 2378-2384; (e) D. Zeng, H. Fang, A. Zheng, J. Xu, L. Chen, J. Yang, J. Wang, C. Ye and F. Deng, *J. Mol. Catal. A: Chemical*, 2007, **270**, 257-263.
- 4 H. S. Fogler, “Elements of Chemical Reaction Engineering”. Prentice- Hall International Editions, (1987).
- 5 D. R. Moberg, T. J. Thibodeau, F. G. Amar and B. G. Frederick, *J. Phys. Chem. C*, 2010, **114**, 13782–13795.
- 6 (a) E. Furimsky, *Appl. Catal. A: Gen.*, 2000, **199**, 147-190; (b) L. Pauling, *The Nature of the Chemical Bond*; Cornell University Press: Ithaca, NY, 1960; (c) P. Atkins and J. de Paula, *Physical Chemistry*, 8th ed.; W.H. Freeman and Company: New York, 2006; (d) S. Li, J. M. Hennigan, D. A. Dixon and K. A. Peterson, *J. Phys. Chem. A*, 2009, **113**, 7861-7877.